



**HAL**  
open science

## A fast and efficient method for the analysis of $\alpha$ -dicarbonyl compounds in aqueous solutions: development and application

Nicolas Brun, Juan Miguel González-Sánchez, Carine Demelas, Jean-Louis Clément, Anne Monod

### ► To cite this version:

Nicolas Brun, Juan Miguel González-Sánchez, Carine Demelas, Jean-Louis Clément, Anne Monod. A fast and efficient method for the analysis of  $\alpha$ -dicarbonyl compounds in aqueous solutions: development and application. *Chemosphere*, 2023, 319, pp.137977. 10.1016/j.chemosphere.2023.137977. hal-04415986

**HAL Id: hal-04415986**

**<https://amu.hal.science/hal-04415986>**

Submitted on 25 Jan 2024

**HAL** is a multi-disciplinary open access archive for the deposit and dissemination of scientific research documents, whether they are published or not. The documents may come from teaching and research institutions in France or abroad, or from public or private research centers.

L'archive ouverte pluridisciplinaire **HAL**, est destinée au dépôt et à la diffusion de documents scientifiques de niveau recherche, publiés ou non, émanant des établissements d'enseignement et de recherche français ou étrangers, des laboratoires publics ou privés.

# 1 A fast and efficient method for the analysis of $\alpha$ -dicarbonyl 2 compounds in aqueous solutions: development and application

3 Nicolas Brun<sup>1,2</sup>, Juan Miguel González-Sánchez<sup>1,2,3</sup>, Carine Demelas<sup>1</sup>, Jean-Louis Clément<sup>2</sup>, Anne  
4 Monod<sup>1</sup>

5 <sup>1</sup>Aix Marseille Univ, CNRS, LCE, Marseille, France

6 <sup>2</sup>Aix Marseille Univ, CNRS, ICR, Marseille, France

7 Now at <sup>3</sup>Aix Marseille Univ, CNRS, MIO, Marseille, France

8

9 Correspondence to: Nicolas Brun ([nicolas.brun@univ-amu.fr](mailto:nicolas.brun@univ-amu.fr)) and Anne Monod ([anne.monod@univ-amu.fr](mailto:anne.monod@univ-amu.fr))

10 Keywords: analytical chemistry, atmospheric chemistry, fogs and clouds chemistry,  $\alpha$ -dicarbonyls, High-Performance Ion  
11 Chromatography

## 12 Abstract.

13 Among the highly oxygenated species formed *in situ* in the atmosphere,  $\alpha$ -dicarbonyl compounds are the most reactive species,  
14 thus contributing to the formation of secondary organic aerosols that affect both air quality and climate. They are ubiquitous  
15 in the atmosphere and are easily transferred to the atmospheric aqueous phase due to their high solubility. In addition,  $\alpha$ -  
16 dicarbonyl compounds are toxic compounds found in food in biochemistry studies as they can be produced endogenously  
17 through various pathways and exogenously through the Maillard reaction. In this work, we take advantage of the high reactivity  
18 of  $\alpha$ -dicarbonyl compounds in alkaline solutions (intramolecular Cannizzaro reaction) to develop an analytical method based  
19 on high performance ion chromatography. This fast and efficient method is suitable for glyoxal, methylglyoxal and  
20 phenylglyoxal which are detected as glycolate, lactate and mandelate anions respectively, with 100% conversion at pH > 12  
21 and room temperature for exposure times to hydroxide ranging from 5 minutes to 4 h. Diacetyl is detected as 2,4-dihydroxy-  
22 2,4-dimethyl-5-oxohexanoate due to a base catalysed aldol reaction that occurs before the Cannizzaro reaction. The analytical  
23 method is successfully applied to monitor glyoxal consumption during aqueous phase HO $\cdot$  oxidation, an atmospherically  
24 relevant reaction using concentrations that can be observed in fog and cloud water. The method also reveals potential analytical  
25 artifacts that can occur in the use of ion chromatography for  $\alpha$ -hydroxy carboxylates measurements in complex matrices due  
26 to  $\alpha$ -dicarbonyl conversion during the analysis time. An estimation of the artifact is given for each of the studied  $\alpha$ -hydroxy  
27 carboxylates. Other polyfunctional and pH-sensitive compounds that are potentially present in environmental samples (such  
28 as nitrooxycarbonyls) can also be converted into  $\alpha$ -hydroxy carboxylates and/or nitrite ions within the HPIC run. This shows  
29 the need for complementary analytical measurements when complex matrices are studied.

## 30 1. Introduction

31 Fast and efficient analysis of small  $\alpha$ -dicarbonyl compounds is essential for atmospheric chemistry, biochemistry and food  
32 chemistry as these compounds are highly reactive, toxic and ubiquitous in the environment. In the atmosphere,  $\alpha$ -dicarbonyl  
33 compounds such as glyoxal, methylglyoxal and diacetyl, are primary and secondary highly reactive compounds. They are  
34 abundant in the gas, aqueous, and particulate phases. They are produced by the gas-phase oxidation of anthropogenic aromatic  
35 hydrocarbons (Volkamer et al., 2001; Calvert et al., 2002; Sato et al., 2012), biogenic terpenes and isoprene (Saunders et al.,  
36 2003; Miller et al., 2016; Wennberg et al., 2018) and can potentially originate from marine biogenic fatty acids (Chiu et al.,  
37 2017). Alpha-dicarbonyl compounds have a high effective Henry's law constant driven by hydrate (gem-diol) formation  
38 (Boreddy and Hoffmann, 1988; Sander, 2015). Therefore, although highly volatile, they partition into the atmospheric aqueous  
39 phase (liquid water droplets and/or wet aerosols), where they undergo a specific reactivity that is very different from that in  
40 the gas phase, the latter being dominated by direct photolysis. Among the most ubiquitous  $\alpha$ -dicarbonyls, glyoxal and  
41 methylglyoxal aqueous-phase reactivity leads to the formation of low- or semi-volatile compounds: they can form oligomers  
42 *via* hemiacetalisation (Loeffler et al., 2006; Avzianova and Brooks, 2013), acid-catalysed aldol condensation (de Haan et al.,  
43 2009a; Nozière et al., 2010) and/or photo-oxidation (Tan et al., 2009; Lee et al., 2011; Zhao et al., 2012). They can be oxidised  
44 to oxalic acid, the dominant dicarboxylic acid in the atmosphere, often observed as the most abundant organic species in  
45 particle matter (Carlton et al., 2007; Tan et al., 2010; Boreddy and Kawamura, 2018). Although the reactivity of diacetyl in  
46 the atmosphere has been much less studied, it has been shown to form light-absorbing products *via* aqueous-phase reactions  
47 with ammonia and/or amines, like glyoxal and methylglyoxal (de Haan et al., 2009b; Kampf et al., 2012; Powelson et al.,  
48 2014; Laskin et al., 2015; Li et al., 2021; Jimenez et al., 2022; Zhang et al., 2022; Faust et al., 1997; Kampf et al., 2016; Grace  
49 et al., 2020). From all these studies,  $\alpha$ -dicarbonyl compounds are likely important atmospheric precursors of Secondary  
50 Organic Aerosols (SOA) that affect both air quality and climate.

51  
52 Alpha-dicarbonyl compounds are also of major interest in food and biochemistry due to their toxicity: they can be generated  
53 endogenously and exogenously (Lange et al., 2012). In food, the Maillard reaction occurs between reducing sugars and amino  
54 acids and produces various  $\alpha$ -dicarbonyl compounds including glyoxal, methylglyoxal and diacetyl (Cha et al., 2019). Previous  
55 studies reveal that  $\alpha$ -dicarbonyls are also precursors of heterocyclic flavour chemicals in the Maillard reaction (Wang and Ho,  
56 2012; Jiang et al., 2013);  $\alpha$ -dicarbonyl compounds have been found in fermented food, dairy products and beverages (Degen  
57 et al., 2012; Wang et al., 2017; Kim et al., 2021). *In vivo*, glyoxal can be formed through various pathways, including  
58 autoxidation of carbohydrates and ascorbate, degradation of glycated proteins and lipid peroxidation (Lange et al., 2012). In  
59 addition,  $\alpha$ -dicarbonyl compounds can modify proteins and form advanced glycation end products, which are related to the  
60 development of many chronic diseases (Lange et al., 2012; Poulsen et al., 2013; Svendsen et al., 2016; Ansari et al., 2018).  
61 Finally,  $\alpha$ -dicarbonyl compounds are cytotoxic and inhibit the function of human enzymes responsible for DNA repair  
62 (Amoroso et al., 2013).

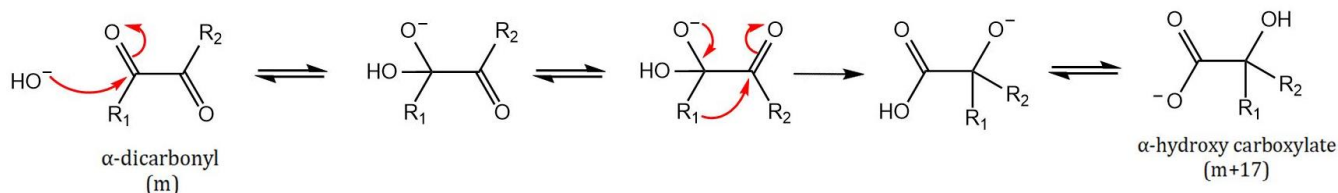
64 Due to their high reactivity, quantitative measurements of  $\alpha$ -dicarbonyl compounds are challenging in aqueous samples.  
65 Indeed, carbonyl compounds promptly hydrate in water, forming gem-diols that are not detectable by spectrophotometry.  
66 Except for diacetyl which can be detected by UV-Visible absorption due to its low hydration in the aqueous phase (Faust et  
67 al., 1997; Zuman, 2002), there are currently no methods for the direct detection and quantification of these compounds in the  
68 liquid phase. The most widely employed methods for the analysis of these compounds use amino trapping reagents to convert  
69  $\alpha$ -dicarbonyl compounds into more stable imine derivative chromophores and/or fluorophores that can be quantified by High-  
70 Performance Liquid Chromatography (HPLC) or Gas Chromatography (GC) coupled to UV detection, fluorimetry or Mass  
71 Spectrometry (MS) (see SI1). The 3 most common amino trapping reagents ((2,3,4,5,6-pentafluorobenzyl)hydroxylamine  
72 (PFBHA), 2,4-dinitrophenylhydrazine (DNPH) and o-phenylenediamine) trap  $\alpha$ -dicarbonyl compounds to produce oximes,  
73 hydrazones and quinoxalines, respectively. However, amino trapping reagents show some disadvantages for the analysis of  $\alpha$ -  
74 dicarbonyl compounds. Undesirable formation of mono-derivatives has been reported (Nakajima et al., 2007). Moreover,  
75 double derivatisation is generally slower than single derivatisation and leads to the formation of three or four isomers  
76 (depending on the symmetry of the  $\alpha$ -dicarbonyl compound). For these reasons, derivatisation using a di-amino compound  
77 such as o-phenylenediamine appears to be more suitable for efficient trapping of  $\alpha$ -dicarbonyl compounds. Furthermore,  
78 although some of the amino trapping reagents are very expensive, they are used in large excess to favour the derivatisation  
79 reaction. The trapping reagents must then be accurately separated from the imine derivatives for quantification. In addition,  
80 the pH of the reaction must be carefully controlled because water elimination in the derivatisation reaction is acid-catalysed  
81 but is also reversible under acidic conditions (Layer, 1963). A too low pH, the reaction can also lead to competitive aldol  
82 condensation of  $\alpha$ -dicarbonyl compounds. Finally, imine derivatives can be poorly water-soluble, affecting the derivatisation  
83 in the case of aqueous solutions.

84

85 In this work, a specific method based on High-Performance Ion Chromatography (HPIC) was developed for a simple, fast and  
86 accessible analysis of  $\alpha$ -dicarbonyl compounds in aqueous solutions. The method has the advantages of high selectivity, high  
87 sensitivity, and simple equipment requirement (Chen et al., 2005). The analytical conditions and performances set by Chen et  
88 al. (2005) for glyoxal were revisited and complemented by MS detection. The method was extended to other  $\alpha$ -dicarbonyl  
89 compounds. Methylglyoxal and diacetyl were selected as they are ubiquitous in the environment, and phenylglyoxal was  
90 chosen as a proxy for aromatic  $\alpha$ -dicarbonyl compounds formed in atmospheric SOA. The developed method was successfully  
91 applied to glyoxal monitoring during its aqueous phase HO $\cdot$ -oxidation under atmospherically realistic conditions. The paper  
92 discusses the advantages of the method as well as potential analytical artifacts that can occur using HPIC for  $\alpha$ -hydroxy  
93 carboxylate measurements in complex aqueous environmental samples.

## 94 2 Materials and methods

95 The method is based on converting  $\alpha$ -dicarbonyl compounds into  $\alpha$ -hydroxy carboxylates in the presence of a strong base *via*  
96 a benzilic acid rearrangement, an intramolecular disproportionation that derives from the Canizzaro reaction (Selman, S., &  
97 Eastham, 1960; Fratzke and Reilly, 1986; Burke and Marques, 2007). The reaction consists of  $\text{HO}^-$  addition, C-C rotation,  
98 carbanion migration, and proton relay towards the produced anions (Fig. 1). The formed  $\alpha$ -hydroxy carboxylates can then be  
99 easily detected using HPIC coupled with conductivity detection and/or mass spectrometry. The chemical conversion can be  
100 performed either by addition of a strong base in the sample before analysis, or into the HPIC system using the mobile phase  
101 with an appropriate NaOH concentration as reagent. In the latter, the measurement of  $\alpha$ -dicarbonyl compounds can be  
102 performed without any conversion process before the analysis and thus allows for direct measurement, but with significantly  
103 lower performances than the former, as shown in the results.



105 **Fig. 1 – General scheme of the chemical conversion of  $\alpha$ -dicarbonyl compounds to  $\alpha$ -hydroxy carboxylates in an alkaline solution**  
106 **(adapted from Yamabe et al., 2006). Each step is reversible, except for the carbanion migration (3<sup>rd</sup> step), which is the rate**  
107 **determining step.**

### 108 2.1 Instrumental setup and operating conditions

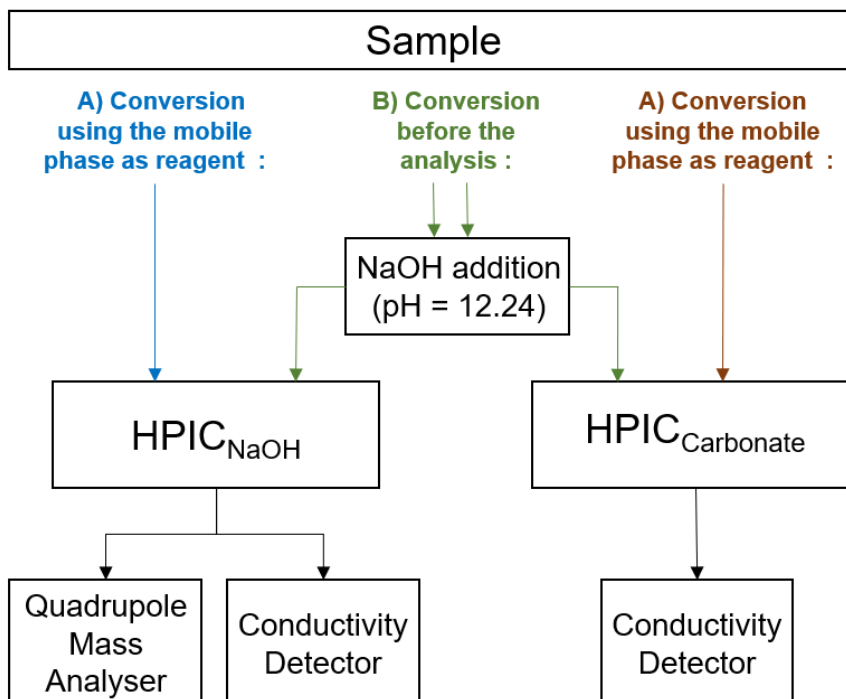
109 Carboxylates were analysed and quantified by two HPIC systems equipped with different mobile phases. The first one was a  
110 Dionex ICS-3000 High-Performance Ion Chromatograph driven by Chromeleon® software. The HPIC was coupled with a  
111 Dionex CD25 Conductivity Detector (CD) in parallel with a Dionex surveyor MSQ mass spectrometer. In each analysis, the  
112 samples were automatically injected using a 100  $\mu\text{L}$  injection loop into a Dionex IonPac AG11-HC precolumn (4 x 50 mm)  
113 connected to a Dionex IonPac AS11-HC column (4 x 250 mm) thermostated at 30  $^{\circ}\text{C}$  with a particle size of 9  $\mu\text{m}$ . The HPIC  
114 was equipped with a Dionex ACRS 500 chemical suppressor with a constant flow of 50 mM  $\text{H}_2\text{SO}_4$  at 3.5  $\text{mL min}^{-1}$ . The MSQ  
115 mass spectrometer was operated in electrospray ionization (ESI) negative mode under a desolvation gas flow of 6  $\text{L min}^{-1}$  at  
116 600  $^{\circ}\text{C}$  and a capillary voltage of 3.5 kV. The sample cone voltage was set at 35 V and carboxylates were detected and  
117 quantified as their deprotonated molecules ( $[\text{M}-\text{H}]^-$ ) with simultaneous full scan and Selected Ion-Monitoring (SIM) for the  
118 targeted  $\alpha$ -hydroxy carboxylates. In each sample, 1  $\text{mg L}^{-1}$  of valeric acid was employed as an internal standard. The injection  
119 volume was 100  $\mu\text{L}$  and the flow rate was 1  $\text{mL min}^{-1}$ . The mobile phase consisted of an aqueous NaOH solution degassed  
120 with purified He and kept under  $\text{N}_2$  atmosphere during the analyses. The separation was performed by isocratic elution. Several  
121 tests were performed using various NaOH concentrations in the mobile phase, ranging from 17.5 to 45 mM (pH range = 12.24  
122 - 12.65), to accelerate the conversion of  $\alpha$ -dicarbonyl compounds within the chromatographic column. This system is further  
123 designated as  $\text{HPIC}_{\text{NaOH}}$ .

124

125 The second HPIC system used comprised a less alkaline mobile phase to study the effect of the mobile phase pH on the  
126 analytical performances. For this purpose, a 761 Compact HPIC System from Metrohm AG was employed including a  
127 Metrosep A Supp 4 (4 x 250 mm) column with a particle size of 5  $\mu\text{m}$ . The system comprised a conductivity detector and a  
128 suppressor module running at a constant flow of 0.5 mL  $\text{min}^{-1}$  of 20 mM  $\text{H}_2\text{SO}_4$ . Samples were manually injected using a 20  
129  $\mu\text{L}$  injection loop. The entire HPIC system was thermostated at 20  $^\circ\text{C}$ . At a flow rate of 1 mL  $\text{min}^{-1}$ , an isocratic method with  
130 a single eluent consisting of an aqueous solution of 2 mM  $\text{NaHCO}_3$  and 1.3 mM  $\text{Na}_2\text{CO}_3$  (pH = 10.14) was used. This system  
131 is further designated as  $\text{HPIC}_{\text{carbonate}}$ .

## 132 2.2 Chemicals and sample preparations

133 All chemicals were commercially available and used as supplied as listed in SI2, except for  $\alpha$ -nitrooxyacetone that was  
134 synthesised following a protocol described in SI3. Conversions of  $\alpha$ -dicarbonyl compounds in alkaline solutions were  
135 performed either into the HPIC system using the mobile phase as reagent (further designated as method A), or before analysis  
136 in amber vials by addition of 17.5 mM NaOH followed by manual shaking for 10 seconds (further designated as method B),  
137 as summarised in Fig. 2. The analyses were systematically complemented with blanks including the UHQ water used for  
138 dilutions, the NaOH solutions used for the conversion reactions and valeric acid as internal standard. Conversion kinetics  
139 experiments were performed using  $\text{HPIC}_{\text{NaOH}}$  by repeatedly sampling the same vials after an initial NaOH addition (at pH =  
140 12.24) and manual shaking for 10 seconds.



141

142 **Fig. 2 – Summary diagram of the various analytical conditions investigated. Samples were converted either using the mobile phase as reagent**  
143 **(method A) or before the analysis (method B) and analysed either by HPIC<sub>NaOH</sub> or by HPIC<sub>Carbonate</sub>.**

## 144 **2.3 Aqueous photooxidation**

145 The study of glyoxal HO $\cdot$ -oxidation in the aqueous phase was performed applying the analytical method developed. The  
146 reaction was performed in a 450 mL batch reactor equipped with Pyrex double wall thermostated at 25°C with ethylene glycol  
147 and covered by a quartz lid. The reactor was irradiated by a Xenon arc lamp 1000 W (LOT Quantum Design) to mimic the  
148 solar irradiance (see SI4). Radiations below 290 nm were filtered by an AM1.5 standard filter (ASTM 892). Homogeneity of  
149 the solution was ensured by magnetic stirring.

150

151 HO $\cdot$  radicals were generated by H<sub>2</sub>O<sub>2</sub> photolysis. In this experiment, H<sub>2</sub>O<sub>2</sub> was monitored by UHPLC-UV analysis (see SI5),  
152 pH and dissolved O<sub>2</sub> were continuously monitored in the solution using specific probes (C3020, Consort, and FDO925, WTW,  
153 respectively). Aliquots were sampled at regular times in amber vials, which quenched the photolysis reaction. Glyoxal and  
154 carboxylate products were analysed from the samples using HPIC<sub>NaOH</sub>. For glyoxal analysis, the samples were five times  
155 diluted and converted before analysis using method B, as described in section 2.2. The photooxidation experiments were  
156 performed at a glyoxal initial concentration of 100  $\mu$ M, about twice higher than the maximum amounts of glyoxal or  
157 methylglyoxal observed in clouds and fogs (Li et al., 2020; Ervens et al., 2013). The initial H<sub>2</sub>O<sub>2</sub> concentration (1 mM) was  
158 chosen to favor by more than 80 % the HO $\cdot$  reaction towards glyoxal over its reaction with H<sub>2</sub>O<sub>2</sub>. A series of control  
159 experiments were performed using HPIC<sub>NaOH</sub>: i) dark reaction of H<sub>2</sub>O<sub>2</sub> with glyoxal (previously reported by Zhao et al., 2012),  
160 ii) direct photolysis of glyoxal (without H<sub>2</sub>O<sub>2</sub>), and iii) direct photolysis of H<sub>2</sub>O<sub>2</sub> (without glyoxal).

## 161 **3 Results and discussions**

### 162 **3.1 Method development**

163 Conversion of  $\alpha$ -dicarbonyl compounds into  $\alpha$ -hydroxy carboxylates through benzilic acid rearrangement is an irreversible  
164 reaction occurring in alkaline medium (Fig. 1) that is highly sensitive to pH (Selman, S., & Eastham, 1960; Gill, 1991; Yamabe  
165 et al., 2006; Wang, 2010). The influence of pH on the analytical method (using HPIC<sub>carbonate</sub> and HPIC<sub>NaOH</sub>) was first studied  
166 in details for glyoxal (in sub-section 3.1.1), then it was applied to methylglyoxal, phenylglyoxal and diacetyl (sub-section 3.1.2).  
167 For each compound, the conversion kinetics were investigated, as well as their conversion proportions (sub-section 3.1.3). The  
168 analytical performances of the method are finally presented in sub-section 3.1.4.

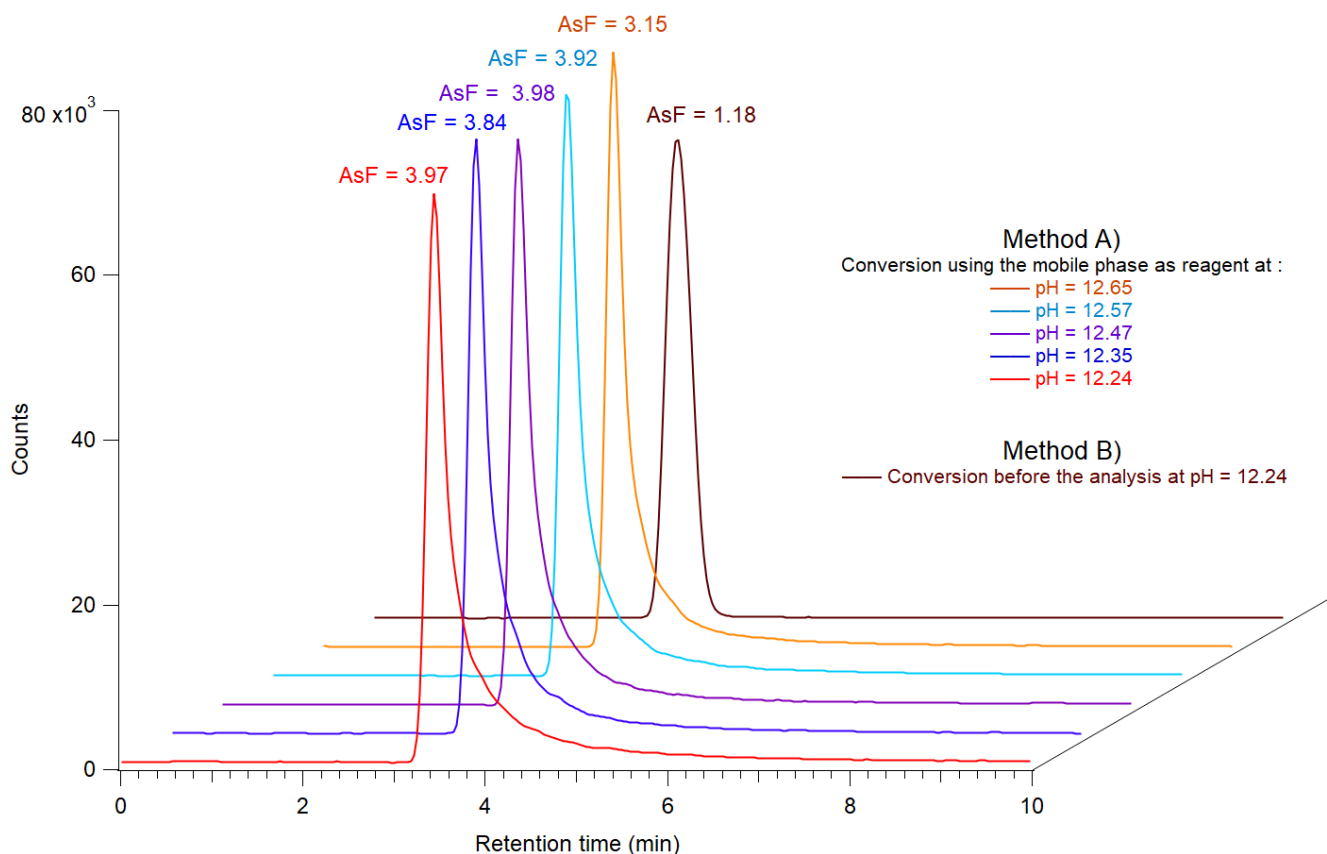
#### 169 **3.1.1 Optimisation of glyoxal analysis**

170 Using method A, no conversion of glyoxal to glycolate was observed using HPIC<sub>carbonate</sub> in contrast to the results obtained  
171 using HPIC<sub>NaOH</sub>. As shown in Fig. 3 a strong glycolate signal was observed using a highly alkaline mobile phase. These results

172 are in very good agreement with the kinetic model of Fratzke and Reilly (1986) which predicts complete conversion of glyoxal  
173 in the analysis timescale (10 min) at pH = 12.24 (conversion half-life of glyoxal < 10 s, see SI6). Glyoxal measurements can  
174 therefore be performed using HPIC<sub>NaOH</sub> without any conversion process before the chromatographic analysis, thus allowing  
175 its direct measurement. However, under these conditions, glycolate quantification was complicated by low-quality  
176 chromatograms due to large peak tailing (Fig. 3). This phenomenon can be explained by the reaction medium successive  
177 conditions encountered by the sample in the HPIC. The reaction started as soon as the sample was in contact with the mobile  
178 phase in the injection loop. When the sample entered the HPIC column, the early formed glycolate molecules were retained,  
179 while the unconverted non-ionic glyoxal molecules were not retained, but were continually converted during the elution  
180 process. The reaction was promoted by the exchangeable counterions of the stationary phase. The reaction then also took place  
181 at the outlet of the column and up to the chemical suppressor where the pH was lowered thus stopping the reaction. Ranging  
182 from 17.5 to 45 mM NaOH concentration as HPIC<sub>NaOH</sub> mobile phase (pH range = 12.24 – 12.65) the asymmetry factor slightly  
183 decreased (Fig. 3) as the reaction rate and elution were accelerated. Nevertheless, the glycolate peak asymmetry factor was  
184 much lower and closer to 1 using method B and HPIC<sub>NaOH</sub> (Fig. 3).

185 Using method B and HPIC<sub>carbonate</sub>, a glycolate signal was also observed showing the irreversibility of the reaction. However,  
186 the strong OH<sup>-</sup> signal due to the high NaOH concentration in the sample and the unsuitable suppressor conditions overlapped  
187 the glycolate signal and resulted in a low-quality chromatogram (not shown).



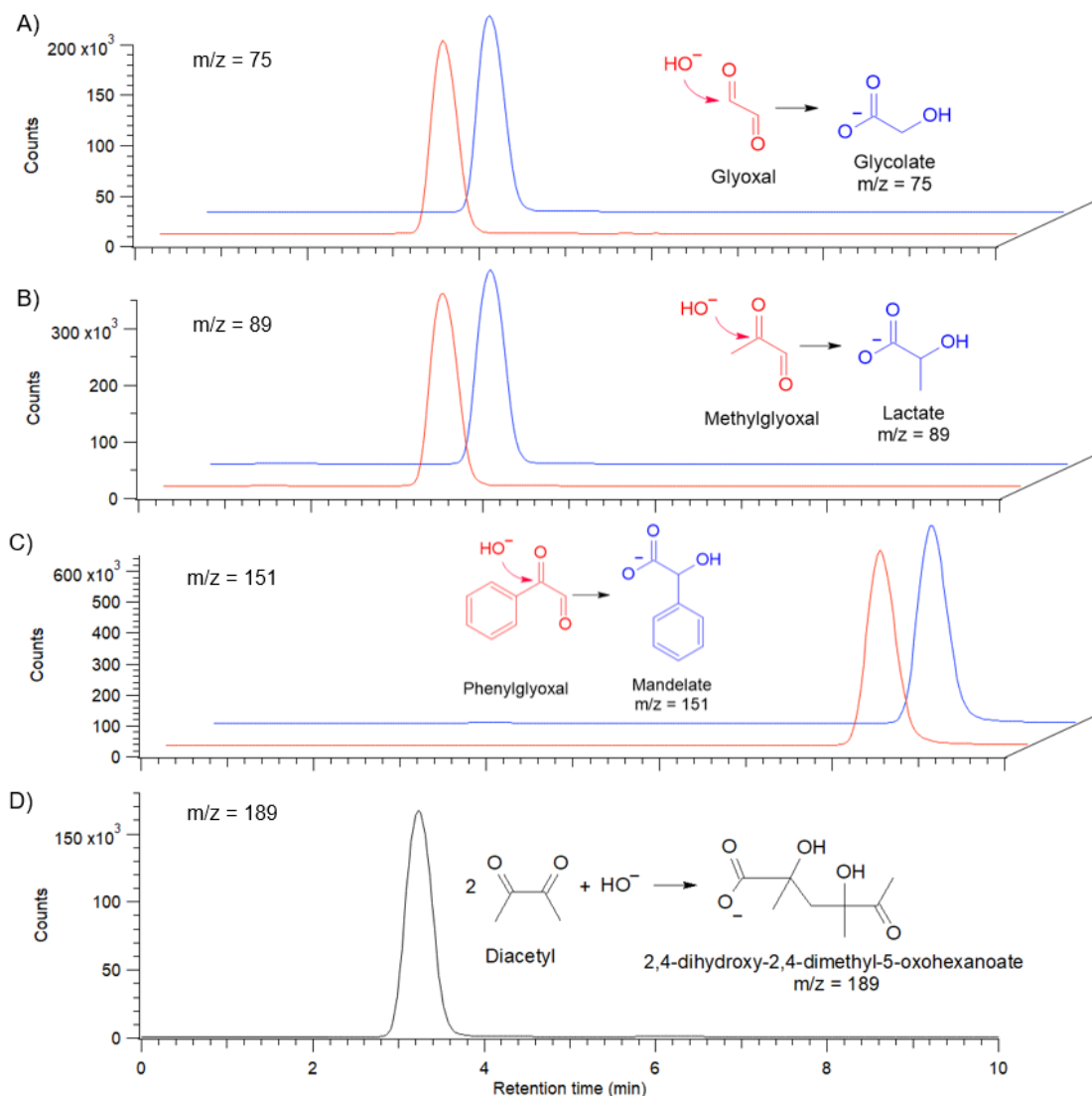


189

190 **Fig. 3 – HPIC<sub>NaOH</sub> SIM chromatograms at  $m/z = 75$  of a  $5 \mu\text{M}$  glyoxal solution using either method B (conversion before the analysis**  
 191 **at pH 12.24), or method A (conversion using the mobile phase as reagent), at various NaOH concentrations, corresponding to the**  
 192 **indicated pH. The peak asymmetry factors (AsF) are indicated at the top of each peak with the corresponding colors. The asymmetry**  
 193 **factor was calculated at 10% of the peak height.**

### 194 3.1.2 Application to other $\alpha$ -dicarbonyl compounds

195 Using method A, as observed for glyoxal, no chemical conversion of methylglyoxal and phenylglyoxal was obtained using  
 196 HPIC<sub>carbonate</sub>, but a strong signal of conversion was observed using HPIC<sub>NaOH</sub>. Under these conditions, lactate and mandelate  
 197 were detected respectively for methylglyoxal and phenylglyoxal, as expected from the mechanism (Fig. 1). However, in the  
 198 same manner as for glyoxal, the chromatograms showed large peak tailing and the deformations were solved using method B  
 199 (Fig. 4). These conversion observations are in very good agreement with the kinetic model predictions of Fratzke and Reilly  
 200 (1986) and Hine et al. (1971), (conversion half-life of methylglyoxal and phenylglyoxal are 7 and 8 min respectively) as  
 201 detailed in SI6.



202

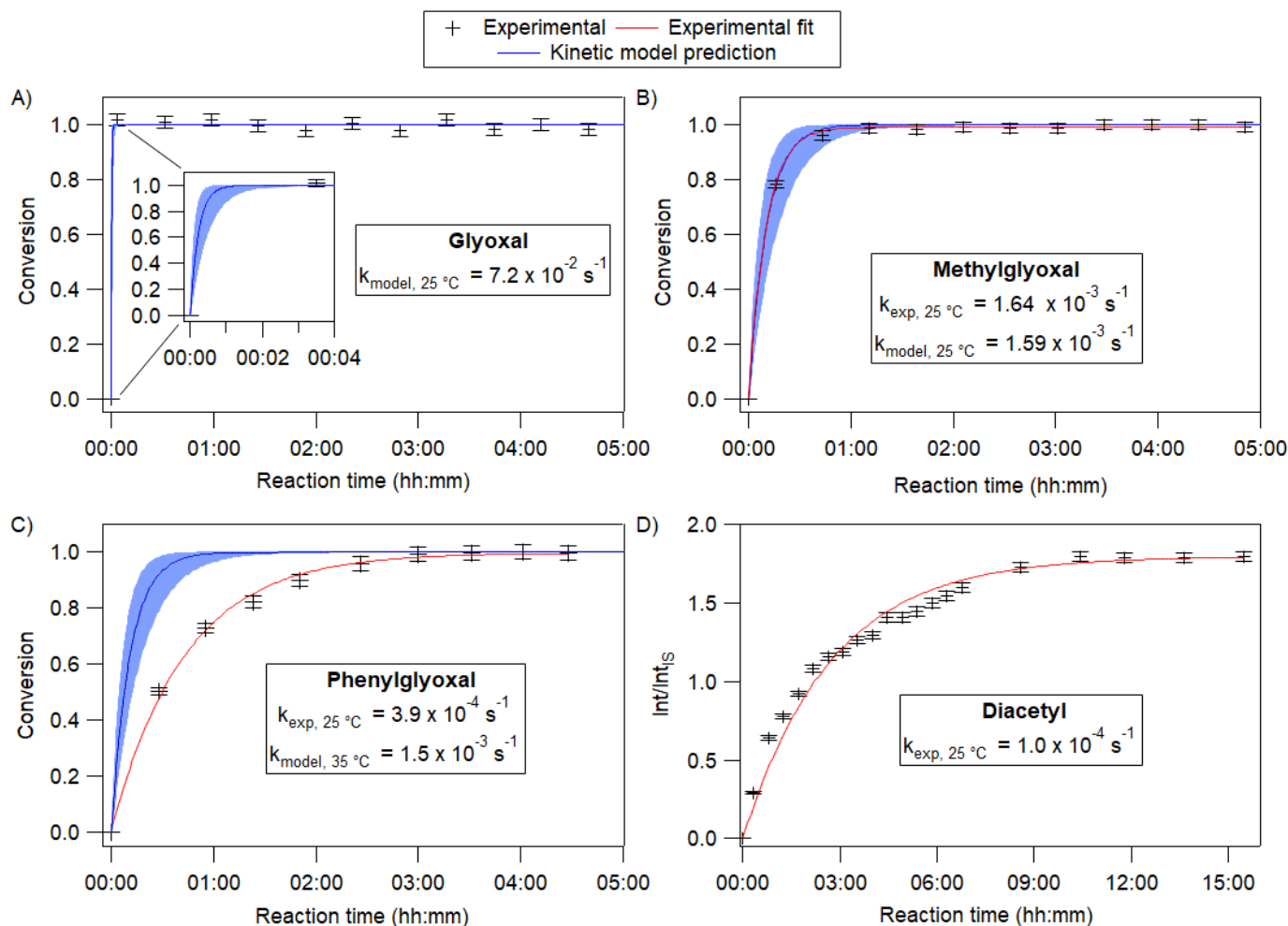
203 **Fig. 4 – HPLC<sub>NaOH</sub> selected-ion monitoring (SIM) chromatograms A) at  $m/z = 75$  of glyoxal (red) and glycolate (blue) solutions B) at**  
 204  **$m/z = 89$  of methylglyoxal (red) and lactate (blue) solutions C) at  $m/z = 151$  of phenylglyoxal (red) and mandelate (blue) solutions.**  
 205 **D) SIM chromatogram at  $m/z = 189$  of a diacetyl solution. The concentration of each compound was 10  $\mu\text{M}$ , the conversion time was**  
 206 **5, 120, 240 and 720 min for glyoxal, methylglyoxal, phenylglyoxal and diacetyl, respectively.**

207 Concerning diacetyl, no signal was detected at  $m/z = 103$  which corresponds to 2-methylactate, expected from the mechanism  
 208 shown in Fig. 1. Instead, a strong signal was observed at  $m/z = 189$  (Fig. 4D) which shows that a more complex chemical  
 209 process occurs under alkaline conditions. This was explained by an additional mechanism shown in Fig. SI7: diacetyl bears  
 210 enolisable hydrogens which allow aldol condensation to compete with the benzilic rearrangement. Diacetyl thus undergoes  
 211 base catalysed aldol condensation and forms an  $\alpha$ -dicarbonyl dimer that is converted to 2,4-dihydroxy-2,4-dimethyl-5-  
 212 oxohexanoate (shown in Fig. 4D) *via* the benzilic acid rearrangement (Machell, 1960). The latter compound is not

213 commercially available, therefore no quantitative comparison with a standard product could be done. Although methylglyoxal  
214 bears enolisable hydrogens on its methyl group as well, no product from a similar mechanism was detected, probably due to  
215 its fast conversion kinetics (see next section) and the smaller number of hydrogens in the molecule.  
216 In summary, the chemical conversion measurement method is also applicable to methylglyoxal, phenylglyoxal and diacetyl  
217 detected as lactate, mandelate and 2,4-dihydroxy-2,4-dimethyl-5-oxohexanoate, respectively, and is more efficient for  
218 quantification using method B than method A.

### 219 3.1.3 Conversion kinetics

220 In addition to being strongly dependent on pH, the conversion kinetics at 25°C were observed to be highly different from one  
221  $\alpha$ -dicarbonyl compound to the other as shown in Fig. 5 where they are compared to the kinetic model predictions proposed by  
222 Fratzke and Reilly (1986) for glyoxal and methylglyoxal and by Hine et al. (1971) for phenylglyoxal. For glyoxal, the  
223 conversion was extremely fast (conversion half-life of glyoxal < 10 s) and reached its maximum within less than 4 minutes.  
224 For methylglyoxal, phenylglyoxal and diacetyl, the conversion kinetics were slower (conversion half-life of methylglyoxal,  
225 phenylglyoxal and diacetyl was 7 min, 29 min and 2 h, respectively) likely because of the more complex mechanisms of the  
226 reaction conversion. In this mechanism (Fig. 1), the migration step of the R<sub>1</sub> group is rate-determining (Yamabe et al., 2006),  
227 therefore, the reaction kinetics depend on the nature of the R<sub>1</sub> and/or R<sub>2</sub> groups. Compared to glyoxal, methylglyoxal and  
228 phenylglyoxal bear a methyl and a phenyl group, respectively, that probably slows down the conversion reaction by steric  
229 hindrance. Furthermore, diacetyl possesses two enolisable methyl groups which allow for more competitive aldol condensation  
230 kinetics. In this case, the conversion reaction occurs after the dimerisation step 1 (Fig. SI7), which likely explains the globally  
231 slower kinetics. Therefore, in addition to low-quality chromatograms, method A results in incomplete conversion of  $\alpha$ -  
232 dicarbonyl compounds with slow conversion kinetics (for methylglyoxal, phenylglyoxal and diacetyl) and thus much lower  
233 performances.



234

235 **Fig. 5 – Temporal evolution of the conversion of A) glyoxal to glycolate (the inner graph shows a zoom in the first 4 minutes), B)**  
 236 **methylglyoxal to lactate, C) phenylglyoxal to mandelate and D) diacetyl to 2,4-dihydroxy-2,4-dimethyl-5-oxohexanoate using SIM**  
 237 **at  $m/z = 75, 89, 103$  and  $151$ , respectively. Chromatographic peak integrated areas (Int) were normalised to integrated areas of**  
 238 **valerate, the internal standard (Int<sub>S</sub>) and compared to the signal of the corresponding  $\alpha$ -hydroxy carboxylate, when possible, to**  
 239 **compute the chemical conversion. Experimental error bars represent the standard deviation between triplicates. Red lines are the**  
 240 **experimental fit using pseudo first-order kinetics:  $1 - \exp(-kt)$ . Blue lines (and shaded blue areas) show the kinetic model prediction**  
 241 **at  $\text{pH} = 12.2 (\pm 0.2)$  set by Fratzke et al. (1986) for glyoxal and methylglyoxal and by Hine et al. (1971) for phenylglyoxal.**

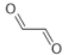
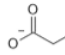
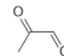
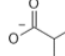
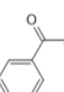
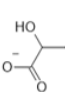
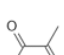
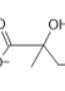
242 Fig. 5 shows that all the experimental kinetics are first-order, in very good agreement with the kinetic results by Hine et al.  
 243 (1971) and Fratzke and Reilly (1986). Using exponential fits, pseudo first-order conversion rate constants of methylglyoxal,  
 244 phenylglyoxal, and diacetyl were respectively  $k_{\text{exp, methylglyoxal}} = 1.6 \times 10^{-3} \text{ s}^{-1}$ ,  $k_{\text{exp, phenylglyoxal}} = 3.9 \times 10^{-4} \text{ s}^{-1}$ ,  $k_{\text{exp, diacetyl}} = 1.0 \times 10^{-4}$   
 245  $\text{s}^{-1}$ . These values are compared in Fig. 5 to the kinetic model predictions developed by Fratzke and Reilly (1986) and Hine et  
 246 al. (1971) that predict  $k$  as a function of  $\text{pH}$  (see SI6). Although no rate constant of glyoxal conversion could be determined in  
 247 this work due to its very fast kinetics under our experimental conditions, Fig. 5 shows excellent agreements between our kinetic  
 248 results and those predicted by Fratzke and Reilly (1986) for glyoxal and methylglyoxal at  $25^{\circ}\text{C}$ . A significantly slower kinetics

249 is observed for phenylglyoxal when compared to the kinetic model prediction by Hine et al. (1971) that was established at 35  
250 °C only. The temperature effect probably explains the kinetic differences observed. Assuming an Arrhenius dependence of the  
251 pseudo first order rate constant of glyoxal conversion and from the work of Fratzke and Reilly (1986), the activation energy  
252 of the glyoxal conversion is 61.2 kJ mol<sup>-1</sup> at pH = 12.24 (see SI8). A rough estimation of the activation energy of the conversion  
253 of phenylglyoxal at pH = 12.24 using the value obtained by Hine et al. (1971) at 35 °C and our rate constant determined at 25  
254 °C results in an activation energy of approximately 100 kJ mol<sup>-1</sup>. Although this value is a rough estimation and should be  
255 confirmed by more experimental data at various temperatures, it is significantly higher than that of glyoxal and may be  
256 explained by steric hindrance due to the phenyl group of the phenylglyoxal.

### 257 **3.1.4 Analytical method performances**

258 The performances were evaluated from the optimal pH and kinetics conditions for each compound using method B, i.e.  
259 conversion before analysis into amber vials at pH > 12 for 5 minutes to 12 h and MS analysis using HPIC<sub>NaOH</sub>. The resulting  
260 SIM chromatograms are shown in Fig. 4. The reaction yield was determined, when possible, at the end of the reaction by  
261 comparison of the  $\alpha$ -hydroxy carboxylate signal in the converted  $\alpha$ -dicarbonyl samples and the signal of authentic  $\alpha$ -hydroxy  
262 carboxylate standard samples, using the two HPIC systems. The performances obtained for the four  $\alpha$ -dicarbonyl compounds  
263 are shown in Table 1. For glyoxal, methylglyoxal and phenylglyoxal the yields were higher than 97 %, whereas no conversion  
264 yield could be derived for diacetyl due to the lack of standard of 2,4-dihydroxy-2,4-dimethyl-5-oxohexanoate. The peak area  
265 of each  $\alpha$ -hydroxy carboxylate showed a good linearity ( $R^2 > 0.99$ ) using concentrations of the corresponding  $\alpha$ -dicarbonyl  
266 compounds ranging from 0.1 to 20  $\mu$ M (see SI9) with good reproducibility (variation coefficient < 2.5 %). No interaction was  
267 observed in mixture samples of the four  $\alpha$ -dicarbonyls and the same values as in single samples were recovered. The detection  
268 limits for the four  $\alpha$ -dicarbonyls ranged from 9 nM to 66 nM (determined using Signal/Noise = 3) and are of the same order  
269 as other recently published results using traditional derivatisation measurement methods (Rodigast et al., 2015). Glyoxal and  
270 methylglyoxal show average concentrations in cloud and fog water ranging respectively from 0.6 to 96  $\mu$ M and from 0.3 to 93  
271  $\mu$ M (Ervens et al., 2013; Li et al., 2020). The method developed in this work thus presents the performances needed by  
272 environmental samples and has the advantage of being simple and fast.

273

$\alpha$ -dicarbonyl			Detected $\alpha$ -hydroxy carboxylate			Analytical performances				
Name	m/z	Structure	Name	m/z	Structure	Yield of the conversion reaction (reaction time)	Linearity ( $R^2$ )	Sensitivity ( $\mu\text{M}^{-1}$ )	Detection limit (nM)	Variation coefficient between triplicates
Glyoxal	58		Glycolate	75		$100 \pm 4\%$ (5 min)	0.9969	0.13	33	2.3%
Methylglyoxal	72		Lactate	89		$97 \pm 5\%$ (2 hrs)	0.9985	0.31	43	1.7%
Phenylglyoxal	134		Mandelate	151		$101 \pm 5\%$ (4 hrs)	0.999	1.16	9	2.5%
Diacetyl	86		2,4-dihydroxy-2,4-dimethyl-5-oxohexanoate	189		not determined	0.9984	0.2	66	1.9%

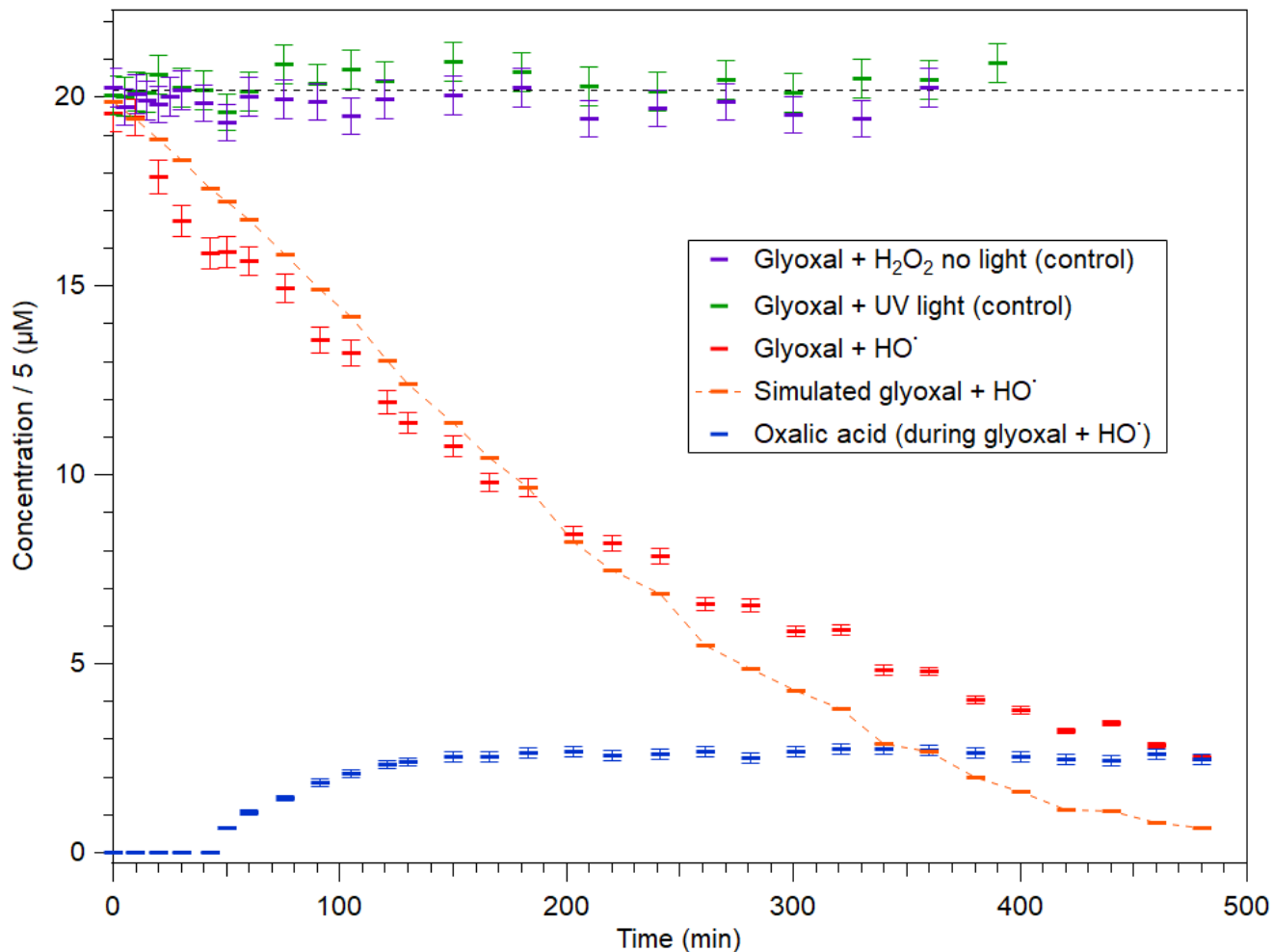
274

275 **Table 1 – Analytical performances of HPIC<sub>NaOH</sub> analysis of  $\alpha$ -dicarbonyl compounds after chemical conversion to  $\alpha$ -hydroxy**  
 276 **carboxylate anions in NaOH solutions at pH>12 (method B).**

### 277 3.2 Application to aqueous phase photooxidation of glyoxal

278 The chemical conversion method for  $\alpha$ -dicarbonyl analysis shows good performances, is simple, fast and requires simple  
 279 instrumentation and cheap solvents. This makes it very suitable for laboratory studies on specific  $\alpha$ -dicarbonyl compounds  
 280 such as aqueous glyoxal  $\cdot\text{OH}$ -oxidation. The results (Fig. 6) show that control experiments revealed no significant direct  
 281 photolysis of glyoxal in the aqueous phase, as expected from glyoxal hydration that suppresses the carbonyl groups and leads  
 282 to the reversible formation of gem-diol, with a high hydration equilibrium constant reached within less than a second (hydration  
 283 half-life of glyoxal is  $< 0.1$  seconds as compiled by Ervens and Volkamer, 2010). This reaction thus prevents the radiation  
 284 absorption by the molecule in water (Montoya and Mellado, 1994). The reaction between glyoxal and  $\text{H}_2\text{O}_2$  reported previously  
 285 (Zhao et al., 2012) was not observed under our experimental conditions, probably due to our low initial concentrations that  
 286 slowed down the formation of hydroxyhydroperoxides. In the presence of  $\text{HO}^\bullet$  radicals (produced from  $\text{H}_2\text{O}_2 + \text{h}\nu$ ), glyoxal  
 287 concentrations decreased exponentially by one order of magnitude within 7h of reaction, while  $\text{H}_2\text{O}_2$  concentrations decreased  
 288 by a factor of 11% (SI10). These kinetics allowed us to derive some values of the rate constants of the limiting reactions, i.e.  
 289  $\text{H}_2\text{O}_2$  direct photolysis  $J_{\text{H}_2\text{O}_2}$ , and glyoxal  $\text{HO}^\bullet$  oxidation  $k_{\text{OH}}$ . Assuming steady state concentrations for  $\text{HO}^\bullet$  and  $\text{HO}_2^\bullet$  radicals,  
 290 the glyoxal and  $\text{H}_2\text{O}_2$  concentration time profiles were simulated using the Microsoft® Excel® Solver routine. Both  $J_{\text{H}_2\text{O}_2}$ , and  
 291  $k_{\text{OH}}$  were optimized to minimize the sum of the square differences between calculated and experimental data (see SI10). The  
 292 results show a good agreement between the simulated and the experimental concentrations (Fig. 6 and SI10), and a value of  
 293  $k_{\text{OH}} = 1.07 \times 10^9 \text{ M}^{-1} \text{ s}^{-1}$  was derived. Although this value is a rough estimation due to the steady state approximations, it is in  
 294 good agreement with the values of  $1.1 \times 10^9$  and  $0.92 \times 10^9 \text{ M}^{-1} \text{ s}^{-1}$  determined by Buxton et al. (1997) and Schaefer et al. (2015)  
 295 respectively. The main photooxidation reaction product detected was secondary oxalic acid, in agreement with previous studies  
 296 (Tan et al., 2009; Lee et al., 2011; Lim et al., 2013; Schaefer et al., 2015). The measurement method developed in this work

297 has thus proven to be simple and efficient to monitor glyoxal during a reaction of atmospheric interest, under concentrations  
298 similar to those observed in clouds and fogs.



299  
300

301 **Fig. 6 – Experimental and simulated glyoxal time profiles during its aqueous phase reaction using SIM at  $m/z = 75$  (glycolate). At**  
302  **$m/z = 89$  oxalate was also monitored as the main secondary reaction product. Error bars represent the standard deviation between**  
303 **analytical triplicates. The samples were diluted by a factor of 5 before analysis.**

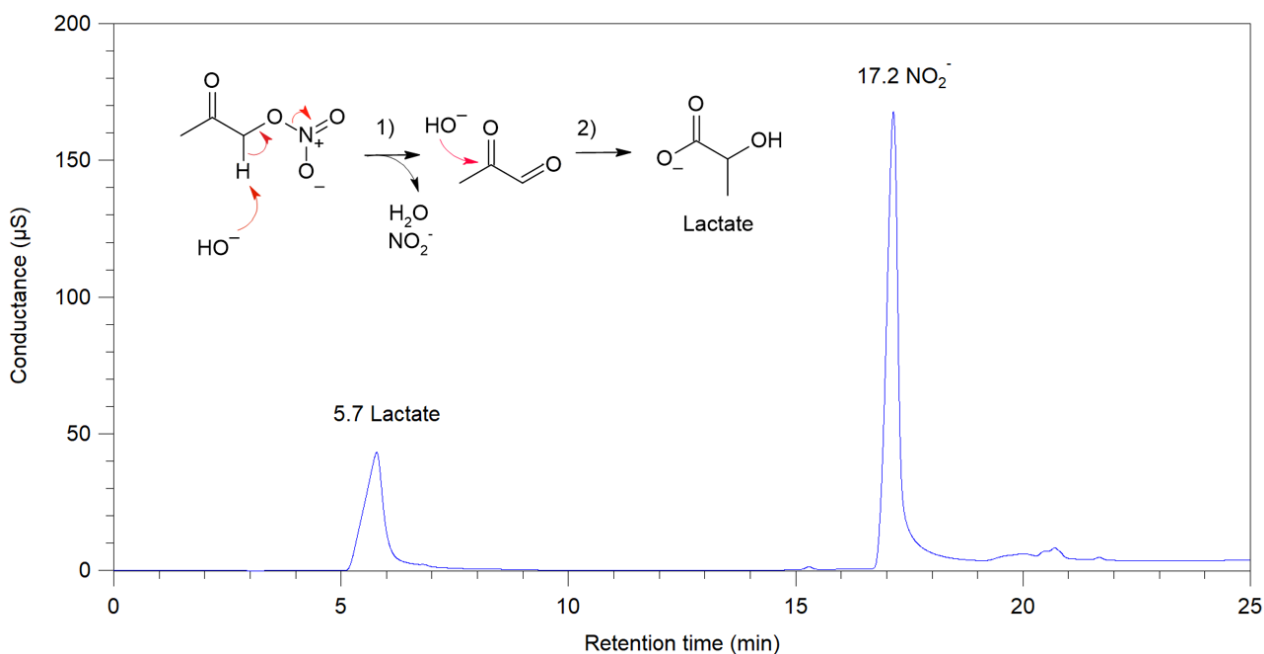
### 304 3.3 Discussions on environmental analysis

305 The method also shows some disadvantages and should therefore be used with caution, especially for complex environmental  
306 samples. Concentrations of  $\alpha$ -dicarbonyls may be overestimated if the samples contain the corresponding  $\alpha$ -hydroxy  
307 carboxylate. In this case, it is necessary to perform a preliminary  $\alpha$ -hydroxy carboxylate quantification at lower pH, to prevent  
308 the conversion of any  $\alpha$ -dicarbonyl compound (see SI11 for more details). For this reason, the method is more suitable for  
309 targeted laboratory studies but remains applicable to environmental samples.

310 Our results also show that the presence of  $\alpha$ -dicarbonyl compounds can induce overestimation biases especially when looking  
311 for organic acids and carboxylates in environmental samples. To evaluate the importance of the conversions that may occur, a  
312 simple calculation was performed for the two most abundant  $\alpha$ -dicarbonyl compounds, glyoxal and methylglyoxal.  
313 Considering the kinetics model proposed by Fratzke and Reilly (1986) and our results, using a typical HPIC method (Wang,  
314 2009) whose pH gradient is often used for environmental analysis, up to 24 and 3% of glyoxal and methylglyoxal can be  
315 converted to their corresponding hydroxy carboxylates respectively. However, the induced biases on the quantification of  $\alpha$ -  
316 hydroxy carboxylates depend on the relative abundance of  $\alpha$ -dicarbonyl to  $\alpha$ -hydroxy carboxylate concentrations in the sample.  
317 Note that other  $\alpha$ -dicarbonyl compounds can also interfere with gluconate, malate, 2-hydroxyvalerate, mucate, tartarate, citrate  
318 and isocitrate measurements. Specific analyses should thus be performed using our methodology (i.e. HPIC<sub>NaOH</sub> and  
319 HPIC<sub>carbonate</sub>) to determine the importance of these biases in environmental samples.

320 Other pH-sensitive compounds can be converted into  $\alpha$ -dicarbonyls and hydroxy-carboxylates during HPIC analysis using  
321 highly alkaline mobile phases, especially compounds prone to base-catalysed hydrolysis. For example, seeking for any  
322 contaminants during the synthesis of  $\alpha$ -nitrooxyacetone, large quantities of lactate and nitrite were detected using HPIC<sub>NaOH</sub>  
323 (see Fig. 7 and SI12 for chromatographic conditions). This phenomenon was explained by the prompt base-catalysed  
324 hydrolysis of  $\alpha$ -nitrooxyacetone that produced nitrite ions and methylglyoxal which was then converted into lactate during the  
325 HPIC<sub>NaOH</sub> analysis (see the mechanism in Fig. 7). Particular care should therefore be taken when performing routine HPIC  
326 analysis of environmental samples which likely contain polyfunctional and pH-sensitive compounds, especially for the  
327 measurement of glycolate, lactate and nitrite ions.

328



329



330 **Fig. 7** HPIC<sub>NaOH</sub> chromatogram of an aqueous solution of  $\alpha$ -nitrooxyacetone. In the figure: Reaction mechanism of  $\alpha$ -  
331 nitrooxyacetone in alkaline medium. 1) Basic hydrolysis 2) Benzilic acid rearrangement.

#### 332 **4. Conclusions**

333 In this work, we took advantage of the high reactivity of  $\alpha$ -dicarbonyl compounds in alkaline solutions (intramolecular  
334 Cannizzaro reaction) to develop an analytical method based on HPIC. The chemical conversion can be performed in the sample  
335 before analysis or in the HPIC system during elution using the mobile phase as reagent. The required mobile phase pH depends  
336 on the targeted  $\alpha$ -dicarbonyl compound, the analysis time and the temperature of the HPIC system. However, when the  
337 chemical conversion was performed using the mobile phase as reagent, chromatographic distortions were observed under our  
338 analytical conditions that were solved by performing the chemical conversion before analysis. When the chemical conversion  
339 was performed before analysis, the analytical method performances were comparable to other recently published traditional  
340 derivatisation methods and allowed for laboratory experiments, such as aqueous phase HO-oxidation of glyoxal, to be  
341 conducted in concentration ranges similar to those observed in the atmosphere. Compared to the previous derivatisation  
342 methods, this alkaline chemical conversion method is much simpler, faster and cheaper but is more suitable for targeted  
343 laboratory experiments. Indeed, potential interferences of  $\alpha$ -hydroxy carboxylates in complex environmental samples can  
344 occur, they need to be treated with caution, for example, using two different elution methods, i.e. mildly alkaline eluents such  
345 as carboxylates and highly alkaline eluents such as sodium or potassium hydroxide solutions.

346

#### 347 **Acknowledgements**

348 The authors acknowledge the support from the French National Research Agency (ANR-PRCI) through the projects  
349 PARAMOUNT (ANR18-CE92-0038-02) and AEROFOG (ANR-22-CE92-0051) and Doctorate school ED251  
350 “Environmental sciences”. The authors would like to thank their colleagues from the laboratory LCE at Aix-Marseille  
351 University, Robert DI ROCCO, who helped with the HPIC<sub>carbonate</sub> analysis, and Etienne Quivet who helped on the choice of  
352 the Journal for paper submission.

#### 353 **References**

354 Amoroso, A., Maga, G., Daglia, M., 2013. Cytotoxicity of  $\alpha$ -dicarbonyl compounds submitted to in vitro simulated digestion  
355 process. Food. Chem. 140(4), 654–659, <https://doi.org/10.1016/j.foodchem.2012.10.063>  
356 Ansari, N. A., Chaudhary, D. K., Dash, D., 2018. Modification of histone by glyoxal: Recognition of glycated histone  
357 containing advanced glycation adducts by serum antibodies of type 1 diabetes patients. Glycobiology. 28(4), 207–213,  
358 <https://doi.org/10.1093/glycob/cwy006>.  
359 Avzianova, E., Brooks, S. D., 2013. Raman spectroscopy of glyoxal oligomers in aqueous solutions. Spectro. Acta A, 101,  
360 40–48, <https://doi.org/10.1016/j.saa.2012.09.050>.

361 Betterton, E. A., Hoffmann, M. R., 1988. Henry's law constants of some environmentally important aldehydes. *Environ. Sci.*  
362 *Technol.* 22(12), 1415-1418.

363 Boreddy, S. K. R., Kawamura, K., 2018. Investigation on the hygroscopicity of oxalic acid and atmospherically relevant  
364 oxalate salts under sub- and supersaturated conditions. *Environ. Sci. Process. Impacts*, 20(7), 1069–1080,  
365 <https://doi.org/10.1039/c8em00053k>

366 Burke, A., Marques, C., 2007. Mechanistic and Synthetic Aspects of the Benzilic Acid and Ester Rearrangements. *Mini-Rev.*  
367 *Org. Chem.* 4(4), 310–316, <https://doi.org/10.2174/157019307782411707>

368 Buxton, G., Malone, T., Arthur Salmon, G., 1997. Oxidation of glyoxal initiated by OH in oxygenated aqueous solution. *J.*  
369 *Chem. Soc., Faraday Transactions*, 93(16), 2889-2891.

370 Calvert, J. G., Atkinson, R., Becker, K. H., Kamens, R. M., Seinfeld, J. H., Wallington, T. H., Yarwood, G., 2002. The  
371 mechanisms of atmospheric oxidation of the aromatic hydrocarbons. Oxford University Press, New York.

372 Carlton, A. G., Turpin, B. J., Altieri, K. E., Seitzinger, S., Reff, A., Lim, H. J., Ervens, B., 2007. Atmospheric oxalic acid and  
373 SOA production from glyoxal: results of aqueous photooxidation experiments. *Atmos. Environ.*, 41(35), 7588–7602,  
374 <https://doi.org/10.1016/j.atmosenv.2007.05.035>

375 Cha, J., Debnath, T., Lee, K. G., 2019. Analysis of  $\alpha$ -dicarbonyl compounds and volatiles formed in Maillard reaction model  
376 systems. *Sci. Rep.*, 9(1), 1–6, <https://doi.org/10.1038/s41598-019-41824-8>

377 Chen, S. P., Huang, T., Sun, S. G., 2005. A new method of ion chromatography technology for speedy determination and  
378 analysis in organic electrosynthesis of glyoxylic acid. *J. Chromatogr. A*, 1089(1-2), 142–147,  
379 <https://doi.org/10.1016/j.chroma.2005.06.076>

380 Chiu, R., Tinel, L., Gonzalez, L., Ciuraru, R., Bernard, F., George, C., Volkamer, R., 2017. UV photochemistry of carboxylic  
381 acids at the air-sea boundary: A relevant source of glyoxal and other oxygenated VOC in the marine atmosphere. *Geophys.*  
382 *Res. Lett.*, 44(2), 1079–1087, <https://doi.org/10.1002/2016GL071240>

383 Degen, J., Hellwig, M., Henle, T., 2012. 1,2-Dicarbonyl compounds in commonly consumed foods. *J. Agric. Food Chem.*,  
384 60(28), 7071–7079, <https://doi.org/10.1021/jf301306g>

385 Ervens, B., Volkamer, R., 2010. Glyoxal processing by aerosol multiphase chemistry: towards a kinetic modeling framework  
386 of secondary organic aerosol formation in aqueous particles. *Atmos. Chem. Phys.*, 10(17), 8219-8244,  
387 <https://doi.org/10.5194/acp-10-8219-2010>

388 Ervens, B., Wang, Y., Eagar, J., Leaitch, W. R., Macdonald, A. M., Valsaraj, K. T., Herckes, P., 2013. Dissolved organic  
389 carbon (DOC) and select aldehydes in cloud and fog water: The role of the aqueous phase in impacting trace gas budgets.  
390 *Atmos. Chem. Phys.*, 13(10), 5117–5135, <https://doi.org/10.5194/acp-13-5117-2013>

391 Faust, B. C., Powell, K., Rao, C. J., Anastasio, C., 1997. Aqueous-phase photolysis of biacetyl (an  $\alpha$ -dicarbonyl compound):  
392 A sink for biacetyl and a source of acetic acid, peroxyacetic acid, hydrogen peroxide, and the highly oxidizing acetylperoxyl  
393 radical in aqueous aerosols, fogs, and clouds. *Atmos. Environ.*, 31(3), 497–510, <https://doi.org/10.1016/S1352->  
394 2310(96)00171-9

395 Fratzke, A. R., Reilly, P. J., 1986. Kinetic analysis of the disproportionation of aqueous glyoxal. *Int. J. Chem. Kinet.*, 18(7),  
396 757–773, <https://doi.org/10.1002/kin.550180704>

397 Gill, G. B. (1991). *Benzil–Benzilic Acid Rearrangements*.

398 de Haan, D. O., Tolbert, M. A., Jimenez, J. L., 2009a. Atmospheric condensed-phase reactions of glyoxal with methylamine.  
399 *Geophys. Res. Lett.*, 36(11), 2–6, <https://doi.org/10.1029/2009GL037441>

400 de Haan, D. O., Corrigan, A. L., Tolbert, M. A., Jimenez, J. L., Wood, S. E., Turley, J. J., 2009b. Secondary organic aerosol  
401 formation by self-reactions of methylglyoxal and glyoxal in evaporating droplets. *Environ. Sci. Technol.*, 43(21), 8184–8190,  
402 <https://doi.org/10.1021/es902152t>

403 Hine, J., Koser, G. F., Koser, G. F., 1971. Kinetics and mechanism of the reaction of phenylglyoxal hydrate with sodium  
404 hydroxide to give sodium mandelate, 36(23), 3591–3593, <https://doi.org/10.1021/jo00822a028>

405 Jiang, Y., Hengel, M., Pan, C., Seiber, J. N., Shibamoto, T., 2013. Determination of toxic  $\alpha$ -dicarbonyl compounds, glyoxal,  
406 methylglyoxal, and diacetyl, released to the headspace of lipid commodities upon heat treatment. *J. Agric. Food. Chem.*, 61(5),  
407 1067–1071, <https://doi.org/10.1021/jf3047303>

408 Jimenez, N. G., Sharp, K. D., Gramyk, T., Uglund, D. Z., Tran, M.-K., Rojas, A., Rafla, M. A., Stewart, D., Galloway, M. M.,  
409 Lin, P., Laskin, A., Cazaunau, M., Pangui, E., Doussin, J.-F., de Haan, D. O., 2022. Radical-initiated brown carbon formation  
410 in sunlit carbonyl–amine–ammonium sulfate mixtures and aqueous aerosol particles. *ACS Earth Space. Chem.*, 6(1), 228–238,  
411 <https://doi.org/10.1021/acsearthspacechem.1c00395>

412 Kampf, C. J., Jakob, R., Hoffmann, T., Ho, T., 2012. Identification and characterization of aging products in the  
413 glyoxal/ammonium sulfate system &ndash; Implications for light-absorbing material in atmospheric aerosols. *Atmos. Chem.*  
414 *Phys.*, 12(14), 6323–6333, <https://doi.org/10.5194/acp-12-6323-2012>

415 Kim, Y., Ahn, H., Lee, K. G., 2021. Analysis of glyoxal, methylglyoxal and diacetyl in soy sauce. *Food. Sci. Biotechnol.*,  
416 30(11), 1403–1408, <https://doi.org/10.1007/s10068-021-00918-8>

417 Lange, J. N., Wood, K. D., Knight, J., Assimos, D. G., Holmes, R. P., 2012. Glyoxal formation and its role in endogenous  
418 oxalate synthesis. *Adv. Urol.*, 2012, 5–10, <https://doi.org/10.1155/2012/819202>

419 Laskin, A., Laskin, J., Nizkorodov, S. A., 2015. Chemistry of atmospheric brown carbon. *Chem. Rev.*, 115(10), 4335–4382,  
420 <https://doi.org/10.1021/cr5006167>

421 Layer, R., 1963. The Chemistry of imines, *Chem. Rev.*, 63, 489–510, <https://doi.org/10.1093/litimag/imq040>

422 Lee, A. K. Y., Zhao, R., Gao, S. S., Abbatt, J. P. D., 2011. Aqueous-phase OH oxidation of glyoxal: Application of a novel  
423 analytical approach employing aerosol mass spectrometry and complementary off-line techniques. *J. Phys. Chem. A*, 115(38),  
424 10517–10526, <https://doi.org/10.1021/jp204099g>

425 Li, T., Wang, Z., Wang, Y., Wu, C., Liang, Y., Xia, M., Yu, C., Yun, H., Wang, W., Wang, Y., Guo, J., Herrmann, H., Wang,  
426 T., 2020. Chemical characteristics of cloud water and the impacts on aerosol properties at a subtropical mountain site in Hong  
427 Kong SAR. *Atmos. Chem. Phys.*, 20(1), 391–407, <https://doi.org/10.5194/acp-20-391-2020>

428 Li, Y., Ji, Y., Zhao, J., Wang, Y., Shi, Q., Peng, J., Wang, Y., Wang, C., Zhang, F., Wang, Y., Seinfeld, J. H., Zhang, R., 2021.  
429 Unexpected oligomerization of small  $\alpha$ -dicarbonyls for secondary organic aerosol and brown carbon formation. *Environ. Sci.*  
430 *Technol.*, 55(8), 4430–4439, <https://doi.org/10.1021/acs.est.0c08066>

431 Lim, Y. B., Tan, Y., Turpin, B. J., 2013. Chemical insights, explicit chemistry, and yields of secondary organic aerosol from  
432 OH radical oxidation of methylglyoxal and glyoxal in the aqueous phase. *Atmos. Chem. Phys.*, 13(17), 8651–8667,  
433 <https://doi.org/10.5194/acp-13-8651-2013>

434 Loeffler, K. W., Koehler, C. A., Paul, N. M., de Haan, D. O., 2006. Oligomer formation in evaporating aqueous glyoxal and  
435 methyl glyoxal solutions. *Environ. Sci. Technol.*, 40(20), 6318–6323, <https://doi.org/10.1021/es060810w>

436 Machell, G., 1960. The action of alkali on diacetyl. *Journal of the Chemical Society (Resumed)*, 683–687.

437 Miller, C. C., Jacob, D., Marais, E., Yu, K., Travis, K., Kim, P., Fisher, J., Zhu, L., Wolfe, G., Keutsch, F., Kaiser, J., Min, K.-  
438 E., Brown, S., Washenfelder, R., González Abad, G., Chance, K., 2017. Glyoxal yield from isoprene oxidation and relation to  
439 formaldehyde: chemical mechanism, constraints from SENEX aircraft observations, and interpretation of OMI satellite data.  
440 *Atmos. Chem. Phys.*, 17(14), 8725-873, <https://doi.org/10.5194/acp-17-8725-2017>

441 Montoya, M. R. Mellado, J. M. R., 1994. Use of convolutive potential sweep voltammetry in the calculation of hydration  
442 equilibrium constants of  $\alpha$ -dicarbonyl compounds. *J. Electroanal. Chem.*, 370(1-2), 183–187, [https://doi.org/10.1016/0022-](https://doi.org/10.1016/0022-0728(93)03203-2)  
443 [0728\(93\)03203-2](https://doi.org/10.1016/0022-0728(93)03203-2)

444 Nozière, B., Dziedzic, P., Córdova, A., 2010. Inorganic ammonium salts and carbonate salts are efficient catalysts for aldol  
445 condensation in atmospheric aerosols. *Phys. Chem. Chem. Phys.*, 12(15), 3864–3872, <https://doi.org/10.1039/b924443c>

446 Poulsen, M. W., Hedegaard, R. v., Andersen, J. M., de Courten, B., Bügel, S., Nielsen, J., Skibsted, L. H., Dragsted, L. O.,  
447 2013. Advanced glycation endproducts in food and their effects on health. *Food chem. toxicol.*, 60, 10–37,  
448 <https://doi.org/10.1016/j.fct.2013.06.052>

449 Powelson, M. H., Espelien, B. M., Hawkins, L. N., Galloway, M. M., de Haan, D. O., 2014. Brown carbon formation by  
450 aqueous-phase carbonyl compound reactions with amines and ammonium sulfate. *Environ. Sci. Technol.*, 48(2), 985–993,  
451 <https://doi.org/10.1021/es4038325>

452 Rodigast, M., Mutzel, A., Inuma, Y., Haferkorn, S., Herrmann, H., 2015. Characterisation and optimisation of a sample  
453 preparation method for the detection and quantification of atmospherically relevant carbonyl compounds in aqueous medium.  
454 *Atmos. Meas. Tech.*, 8(6), 2409–2416, <https://doi.org/10.5194/amt-8-2409-2015>

455 Sander, R., 2015. Compilation of Henry's law constants (version 4.0) for water as solvent. *Atmos. Chem. Phys.*, 15(8), 4399–  
456 4981, <https://doi.org/10.5194/acp-15-4399-2015>

457 Sato, K., Takami, A., Kato, Y., Seta, T., Fujitani, Y., Hikida, T., Shimono, A., Imamura, T., 2012. AMS and LC/MS analyses  
458 of SOA from the photooxidation of benzene and 1,3,5-trimethylbenzene in the presence of NO<sub>x</sub>: Effects of chemical structure  
459 on SOA aging. *Atmos. Chem. Phys.*, 12(10), 4667–4682, <https://doi.org/10.5194/acp-12-4667-2012>

460 Saunders, S. M., Jenkin, M. E., Derwent, R. G., Pilling, M. J., 2003. Protocol for the development of the Master Chemical  
461 Mechanism, MCM v3 (Part A): Tropospheric degradation of non-aromatic volatile organic compounds. *Atmos. Chem. Phys.*,  
462 3(1), 161–180, <https://doi.org/10.5194/acp-3-161-2003>

463 Schaefer, T., van Pinxteren, D., Herrmann, H., 2015. Multiphase chemistry of glyoxal: Revised kinetics of the alkyl radical  
464 reaction with molecular oxygen and the reaction of glyoxal with OH, NO<sub>3</sub>, and SO<sub>4</sub><sup>-</sup> in aqueous solution. *Environ. Sci.*  
465 *Technol.*, 49(1), 343–350, <https://doi.org/10.1021/es505860s>

466 Selman, S., & Eastham, J. F., 1960. Benzilic acid and related rearrangements, 14(3), 221–235, <https://doi.org/10.1093/nq/s3->  
467 IV.94.316-a

468 Svendsen, C., Høie, A. H., Alexander, J., Murkovic, M., Husøy, T., 2016. The food processing contaminant glyoxal promotes  
469 tumour growth in the multiple intestinal neoplasia (Min) mouse model. *Food chem. toxicol.*, 94, 197–202,  
470 <https://doi.org/10.1016/j.fct.2016.06.006>

471 Tan, Y., Perri, M. J., Seitzinger, S. P., Turpin, B. J., 2009. Effects of precursor concentration and acidic sulfate in aqueous  
472 glyoxal - OH radical oxidation and implications for secondary organic aerosol. *Environ. Sci. Technol.*, 43(21), 8105–8112,  
473 <https://doi.org/10.1021/es901742f>

474 Tan, Y., Carlton, A. G., Seitzinger, S. P., Turpin, B. J., 2010. SOA from methylglyoxal in clouds and wet aerosols:  
475 Measurement and prediction of key products. *Atmos. Environ.*, 44(39), 5218–5226,  
476 <https://doi.org/10.1016/j.atmosenv.2010.08.045>

477 Volkamer, R., Platt, U., Wirtz, K., 2001. Primary and secondary glyoxal formation from aromatics: Experimental evidence for  
478 the bicycloalkyl - radical pathway from benzene, toluene, and p-xylene. *J. Phys. Chem. A*, 105(33), 7865–7874,  
479 <https://doi.org/10.1021/jp010152w>

480 Wang, C., Lu, Y., Huang, Q., Zheng, T., Sang, S., Lv, L., 2017. Levels and formation of  $\alpha$ -dicarbonyl compounds in beverages  
481 and the preventive effects of flavonoids. *J. Food Sci. Technol.*, 54(7), 2030–2040, <https://doi.org/10.1007/s13197-017-2639-z>

482 Wang, L., 2009. Determination of 32 low molecular mass organic acids in biomass by ion chromatography mass spectrometry.

483 Wang, Y. Ho, C. T., 2012. Flavour chemistry of methylglyoxal and glyoxal. *Chem. Soc. Rev.*, 41(11), 4140–4149,  
484 <https://doi.org/10.1039/c2cs35025d>

485 Wennberg, P. O., Bates, K. H., Crouse, J. D., Dodson, L. G., McVay, R. C., Mertens, L. A., Nguyen, T. B., Praske, E.,  
486 Schwantes, R. H., Smarte, M. D., St Clair, J. M., Teng, A. P., Zhang, X., Seinfeld, J. H., 2018. Gas-phase reactions of isoprene  
487 and its major oxidation products. *Chem. Rev.*, 118(7), 3337–3390, <https://doi.org/10.1021/acs.chemrev.7b00439>

488 Yamabe, S., Tsuchida, N., Yamazaki, S., 2006. A FMO-controlled reaction path in the benzil-benzilic acid rearrangement. *J.*  
489 *Org. Chem.*, 71(5), 1777–1783, <https://doi.org/10.1021/jo051862r>

490 Zhang, R., Gen, M., Liang, Z., Li, Y. J., Chan, C. K., 2022. Photochemical reactions of glyoxal during particulate ammonium  
491 nitrate photolysis: brown carbon formation, enhanced glyoxal decay, and organic phase formation. *Environ. Sci. Technol.*,  
492 56(3), 1605–1614, <https://doi.org/10.1021/acs.est.1c07211>

493 Zhao, R., Lee, A. K. Y., Abbatt, J. P. D., 2012. Investigation of aqueous-phase photooxidation of glyoxal and methylglyoxal  
494 by aerosol chemical ionization mass spectrometry: observation of hydroxyhydroperoxide formation. *J. Phys. Chem. A*,  
495 116(24), 6253–6263, <https://doi.org/10.1021/jp211528d>  
496 Zuman, P., 2002. Additions of water, hydroxide ions, alcohols and alkoxide ions to carbonyl and azomethine bonds. *Arkivoc*,  
497 1, 85–140, <https://doi.org/10.3998/ark.5550190.0003.114>  
498